


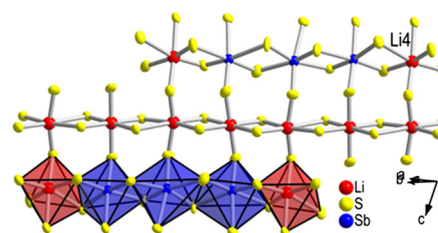
# The fourfold superstructure in $\text{Li}_3\text{Sb}_{11}\text{S}_{18}$

Sebastian Huber<sup>1</sup> · Arno Pfitzner<sup>1</sup> 

Received: 10 August 2017 / Accepted: 9 October 2017 / Published online: 18 January 2018  
© Springer-Verlag GmbH Austria 2018

**Abstract**  $\text{Li}_3\text{Sb}_{11}\text{S}_{18}$  was synthesized by a solid-state reaction of stoichiometric amounts of  $\text{Li}_2\text{S}$  and  $\text{Sb}_2\text{S}_3$ . The crystal structure was determined from dark-gray single crystals at 123 K.  $\text{Li}_3\text{Sb}_{11}\text{S}_{18}$  crystallizes in the triclinic space group  $P\bar{1}$  with  $a = 8.871(1)$  Å,  $b = 11.993(1)$  Å,  $c = 15.407(1)$  Å,  $\alpha = 80.014(5)^\circ$ ,  $\beta = 73.599(5)^\circ$ ,  $\gamma = 77.443(5)^\circ$ ,  $V = 1523.9(2)$  Å<sup>3</sup>, and  $Z = 2$  (data at 123 K). Both metals have a distorted octahedral coordination by sulfur. These octahedra are arranged in two different types of alternating layers. Strands of *trans* edge sharing octahedra  $\text{LiS}_6$  and octahedra  $\text{SbS}_6$  form heterocubane units  $\text{LiSb}_3\text{S}_4$ , which are condensed to a rock salt type layer one. Layer two consists mainly of  $\text{SbS}_6$ -units also packed in a rock salt motif. Some of the antimony atoms are replaced by lithium in a systematic way. In total, a deficient rock salt type structure results for  $\text{Li}_3\text{Sb}_{11}\text{S}_{18}$ .

## Graphical abstract



**Keywords** Ion conductor · Electrode material · Crystal structure · Lithium · Thioantimonate

## Introduction

The phase diagram  $\text{Li}_2\text{S}$ – $\text{Sb}_2\text{S}_3$  was first studied in 1983 with differential thermal analysis (DTA) measurements and X-ray diffraction by Olivier-Fourcade et al. [1, 2]. They characterized therein the high-temperature modification of  $\text{LiSbS}_2$ ,  $\text{Li}_{1.5}\text{Sb}_{5.5}\text{S}_9$ , and  $\text{Li}_{0.999}\text{Sb}_{5.667}\text{S}_9$  by single-crystal structure determination and further ternary compounds, e.g.,  $\text{Li}_3\text{SbS}_3$  and  $\text{Li}_6\text{Sb}_4\text{S}_9$  by X-ray powder diffraction. During systematic investigations for new lithium ion conductors, we recently reinvestigated the phase diagram  $\text{Li}_2\text{S}$ – $\text{Sb}_2\text{S}_3$  and determined the crystal structures of  $\text{Li}_3\text{SbS}_3$ ,  $\text{Li}_{17}\text{Sb}_{13}\text{S}_{28}$ , and  $\text{LiSbS}_2$ -*mC16* [3–5].  $\text{Li}_{17}\text{Sb}_{13}\text{S}_{28}$  turned out to be the formerly postulated “ $\text{Li}_6\text{Sb}_4\text{S}_9$ ”, and  $\text{LiSbS}_2$ -*mC16* is the low-temperature modification of  $\text{LiSbS}_2$ . Besides these lithium-rich compounds in the system  $\text{Li}_2\text{S}$ – $\text{Sb}_2\text{S}_3$ , which are interesting as solid electrolytes, the end member  $\text{Sb}_2\text{S}_3$  is discussed as an electrode material for novel high-performance

**Electronic supplementary material** The online version of this article (<https://doi.org/10.1007/s00706-017-2072-z>) contains supplementary material, which is available to authorized users.

Dedicated to Prof. Thomas Schleid on the Occasion of his 60th Birthday.

✉ Arno Pfitzner  
arno.pfitzner@chemie.uni-regensburg.de

<sup>1</sup> Institut für Anorganische Chemie, Universität Regensburg, 93040 Regensburg, Germany

rechargeable batteries [6–8]. To date only limited structural information is available on the compounds formed during the reaction of small amounts of  $\text{Li}_2\text{S}$  with  $\text{Sb}_2\text{S}_3$  [2]. Herein, we report on the synthesis and structure determination of  $\text{Li}_3\text{Sb}_{11}\text{S}_{18}$ , which is an ordered variant of  $\text{Li}_{1.5}\text{Sb}_{5.5}\text{S}_9$ .

**Table 1** Crystallographic data for the structure analysis of  $\text{Li}_3\text{Sb}_{11}\text{S}_{18}$

Compound	$\text{Li}_3\text{Sb}_{11}\text{S}_{18}$
Formula weight/ $\text{g mol}^{-1}$	1937.2
Color	Dark-gray
Crystal system	Triclinic
Space group	$P\bar{1}$ (no. 2)
Lattice parameters/ $\text{\AA}$	
$a$	8.871 (1)
$b$	11.993 (1)
$c$	15.407 (1)
And angles/ $^\circ$	
$\alpha$	80.014 (5)
$\beta$	73.599 (5)
$\gamma$	77.443 (5)
Cell volume $V/\text{\AA}^3$	1523.9 (2)
Number of formula units per unit cell $Z$	2
Calculated density $\rho_{\text{calc}}/\text{g cm}^{-3}$	4.222
Temperature $T/\text{K}$	123
Wavelength $\lambda/\text{\AA}$	0.71073
Diffractometer	Oxford Diffraction SuperNova
Absorption coeff. $\mu(\text{MoK}\alpha)/\text{mm}^{-1}$	10.82
Absorption correction	Gaussian [25]
$2\theta$ range/ $^\circ$	$6.2 \leq 2\theta \leq 52.7$
$hkl$ ranges	$-11 \leq h \leq 11$ $-14 \leq k \leq 14$ $-19 \leq l \leq 18$
No. of reflections, $R_{\text{int}}$	9442, 0.054
No. of independent reflections	6182
Structure solution	SuperFlip [26]
Structure refinement	Jana 2006 [27]
No. of parameters	271
Final $R$ , $wR$ ( $I > 2\sigma(I)$ )	0.044, 0.057
Final $R$ , $wR$ (all reflections)	0.075, 0.067
GooF	1.09
Largest difference peak $\Delta\rho_{\text{max}}$	1.94
And hole $\Delta\rho_{\text{min}}/\text{e \AA}^{-3}$	$-2.16$

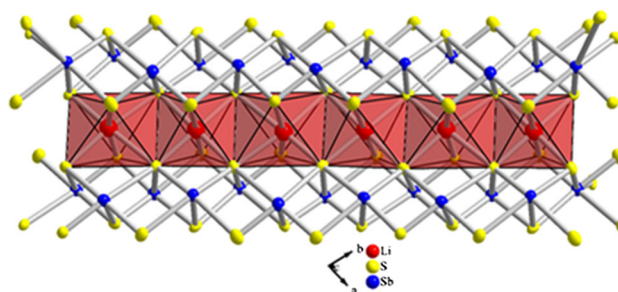
Further details on the crystal structure investigations may be obtained from the Fachinformationszentrum Karlsruhe, 76344 Eggenstein-Leopoldshafen, Germany (Fax: (+49)7247-808-666; E-mail: crys-data@fiz-karlsruhe.de), on quoting the depository number CSD-433665

## Results and discussion

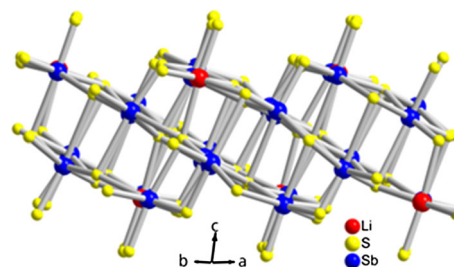
The crystal structure of  $\text{Li}_3\text{Sb}_{11}\text{S}_{18}$  was determined by single-crystal X-ray diffraction at 123 K.  $\text{Li}_3\text{Sb}_{11}\text{S}_{18}$  crystallizes in the triclinic space group  $P\bar{1}$  with  $a = 8.871(1) \text{ \AA}$ ,  $b = 11.993(1) \text{ \AA}$ ,  $c = 15.407(1) \text{ \AA}$ ,  $\alpha = 80.014(5)^\circ$ ,  $\beta = 73.599(5)^\circ$ ,  $\gamma = 77.443(5)^\circ$ ,  $V = 1523.9(2) \text{ \AA}^3$ , and  $Z = 2$  (data at 123 K), see Table 1 for details. Atomic positions, anisotropic displacement parameters, and interatomic distances are provided in Tables S1–S3. The structure of  $\text{Li}_3\text{Sb}_{11}\text{S}_{18}$  is built up by two different types of layers alternating along [001]. Layer one is a section of a rock salt type structure. It consists of chains of edge sharing  $\text{LiS}_6$ -octahedra in [110], which are formed by Li1, Li2, and Li3. Antimony and sulfur complete heterocubane like units  $\text{LiSb}_3\text{S}_4$ , see Fig. 1.

Layer two exhibits four planes of metal atoms; both antimony and lithium show a distorted octahedral coordination by sulfur, see Fig. 2. The lithium content of this layer is significantly smaller than that of the layer one, and lithium is located in only a few peripheral octahedral sites at the borders of these layers (Li4), which are isolated from each other.

The octahedra are distorted in a systematic manner. Thus, sixfold coordination results for Li1 and Li2 with distances  $d(\text{Li-S}) = 2.4\text{--}2.8 \text{ \AA}$ , whereas Li3 and Li4 have a  $5 + 1$  coordination [ $d_{\text{max}}(\text{Li-S}) = 3.2 \text{ \AA}$ ]. All antimony



**Fig. 1** Edge sharing octahedra  $\text{LiS}_6$  are forming strands in the layers of type 1. Heterocubane-like fragments are completed by Sb and S



**Fig. 2** Layers of type 2 exhibit a rock salt type structure consisting of octahedra  $\text{SbS}_6$  in the central part of the layer and some octahedra  $\text{LiS}_6$  in the border region

**Table 2** Primary and secondary distances [ $d(\text{Sb}-\text{S})$ ] in  $\text{Li}_3\text{Sb}_{11}\text{S}_{18}$ , see Table S3 for all distances

	$d(\text{Sb}-\text{S})/\text{\AA}$	$d_{\text{sec}}(\text{Sb}-\text{S})/\text{\AA}$
Sb1	2.39–2.53	3.22–3.48
Sb2	2.49–2.52	3.05–3.21
Sb3	2.47–2.54	3.09–3.48
Sb4	2.46–2.57	3.02–3.46
Sb5	2.46–2.77	3.25–3.31
Sb6	2.51–2.55	3.00–3.39
Sb7	2.43–2.50	3.13–3.33
Sb8	2.48–2.55	3.09–3.38
Sb9	2.47–2.63	2.93–3.42
Sb10	2.42–2.58	3.11–3.54
Sb11	2.48–2.60	3.02–3.15

Note that the distances are determined much more precisely, but these data are not shown here for the sake of clarity

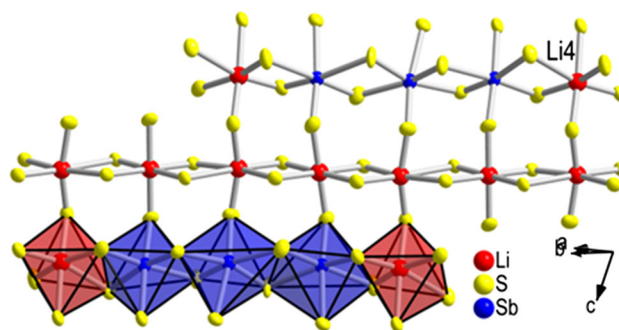
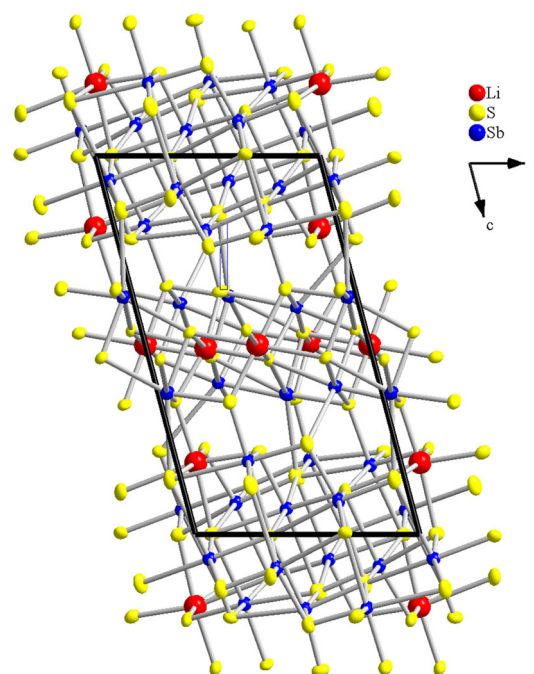
atoms exhibit a  $3 + 3$  coordination mode with distances  $d(\text{Sb}-\text{S}) = 2.39\text{--}2.77\text{ \AA}$  and  $d_{\text{sec}}(\text{Sb}-\text{S}) = 2.93\text{--}3.54\text{ \AA}$ , see Table 2. These secondary bonds are typical for antimony(III) with a coordination number  $> 3$  [9–11]. The coordination numbers for sulfur range from 3 to 6 due to the interconnection of the two different layers along  $c$ . It has to be mentioned that  $\text{Li}^+$  and  $\text{Sb}^{3+}$  have an identical ion radius of  $0.76\text{ \AA}$  according to Shannon [12]. Thus, the expected interatomic distances  $d(M-\text{S})$  are  $2.6\text{ \AA}$  for both metals  $M$  and a regular coordination. However,  $\text{Sb}^{3+}$  shows larger deviations from a regular octahedral coordination than  $\text{Li}^+$  with minimum angles  $< (\text{S}-\text{Sb}-\text{S}) 69^\circ$ , instead of  $90^\circ$  and  $149^\circ$  instead of  $180^\circ$ , respectively. The angles  $< (\text{S}-\text{Li}-\text{S})$  with the largest deviations are  $77^\circ$  and  $164^\circ$ , respectively.

It turns out that the unit cell volume of  $\text{Li}_3\text{Sb}_{11}\text{S}_{18}$  is four times larger than that of  $\text{Li}_{1.5}\text{Sb}_{5.5}\text{S}_9$  [2], see Table 3. At that time, the authors postulated a statistical disorder of 75% antimony and 25% lithium in layer two (Li4 in our structural data). We could now solve the fourfold superstructure, see Figs. 3 and 4.

**Table 3** Comparison of the lattice constants of  $\text{Li}_3\text{Sb}_{11}\text{S}_{18}$  and  $\text{Li}_{1.5}\text{Sb}_{5.5}\text{S}_9$ 

	$\text{Li}_3\text{Sb}_{11}\text{S}_{18}$	$\text{Li}_{1.5}\text{Sb}_{5.5}\text{S}_9$
Space group	$P\bar{1}$	$P\bar{1}$
$a/\text{\AA}$	8.871(1)	4.091(1)
$b/\text{\AA}$	11.993(1)	6.638(2)
$c/\text{\AA}$	15.407(1)	14.769(4)
$\alpha/^\circ$	80.014(5)	96.70(2)
$\beta/^\circ$	73.599(5)	90.79(2)
$\gamma/^\circ$	77.443(5)	107.47(2)
$V/\text{\AA}^3$	1523.9(2)	379.45

Data for  $\text{Li}_{1.5}\text{Sb}_{5.5}\text{S}_9$  are taken from [2]

**Fig. 3** Li4 and Sb atoms with an octahedral coordination are arranged in an ordered way and thus are forming the fourfold superstructure of the title compound**Fig. 4** Projection of the crystal structure of  $\text{Li}_3\text{Sb}_{11}\text{S}_{18}$  along [010]. The two different layers are stacked along [001]

The crystal structure determination of the title compound provides some more insight into the structural chemistry of the compounds in the system  $\text{Li}_2\text{S}-\text{Sb}_2\text{S}_3$ . A strong tendency of the ternary compounds therein to form crystal structures with more or less distorted octahedral environments of the cations is observed. Starting from  $\text{Li}_2\text{S}$ , which crystallizes in the anti-fluorite structure type and provides a tetrahedral surrounding for Li, the most Li-rich compound  $\text{Li}_3\text{SbS}_3$  [3] already shows the tendency of lithium to prefer an increasing coordination number (with one Li in a  $5 + 1$  coordinated site). Despite the almost identical ionic radii of  $\text{Li}^+$  and  $\text{Cu}^+$ , the coordination behavior of these two cations is quite different. A comparison of the crystal structures of  $\text{Li}_3\text{SbS}_3$  and  $\text{Cu}_3\text{SbS}_3$  [13–15] shows a quite similar thioantimonate(III)

framework. Nevertheless, the coordination behavior of  $\text{Cu}^+$  with coordination numbers smaller or equal four leads to significantly different structures, regardless of the different polymorphs formed by  $\text{Cu}_3\text{SbS}_3$ . The major reason is certainly the fact that  $\text{Cu}^+$  avoids an octahedral environment, whereas  $\text{Li}^+$  shows a strong preference for this coordination. Systematic studies of a number of ion conducting materials revealed that even in case of mobile lithium and copper ions a strong site preference has to be taken into account [16, 17]. Hence,  $\text{Cu}^+$  and  $\text{Li}^+$  occupy one common site at low temperature, but  $\text{Li}^+$  changes its environment at elevated temperatures. However, the ion mobility seems to be closely related to  $\text{Li}^+$  ions partially located in a tetrahedral surrounding.

The increased antimony content and the smaller ratio of the number of cations per anion in  $\text{Li}_{17}\text{Sb}_{13}\text{S}_{28}$  [4] already leads to the formation of an ordered rock salt-like structure with strong distortions and vacancies in the anionic substructure. Thus, two vacancies are ordered such that they are surrounded exclusively by  $\text{Sb}^{3+}$  cations, suggesting an interaction of the lone electron pairs of these cations. Further increased antimony content in this series of compounds is found in  $\text{LiSbS}_2$ -*cF8* [1, 2]. The high-temperature modification is of the rock salt structure type with  $\text{Li}^+$  and  $\text{Sb}^{3+}$  disordered on one common position. However, the preference of  $\text{Sb}^{3+}$  for an asymmetric coordination sphere of sulfur leads to the formation of an ordered and distorted modification  $\text{LiSbS}_2$ -*mC16* [3]. Therein, two long distances  $d(\text{Sb}-\text{S}) > 3.2 \text{ \AA}$  are observed, whereas four shorter distances range from 2.45 to 2.77  $\text{\AA}$ . The environment of  $\text{Li}^+$  is more regular with six distances  $d(\text{Li}-\text{S})$  in the range from 2.65 to 2.9  $\text{\AA}$ .

The ratio of the number of cations per anion in  $\text{Li}_3\text{Sb}_{11}\text{S}_{18}$  is 2.33/3, i.e., it is close to the ratio in  $\text{Sb}_2\text{S}_3$ . Therefore, one can expect a coordination behavior of  $\text{Sb}^{3+}$  similar to that observed in  $\text{Sb}_2\text{S}_3$ . Two different  $\text{Sb}^{3+}$  cations therein have a significantly different coordination sphere [18]. The stereoactivity of the lone electron pair of  $\text{Sb}^{3+}$  becomes obvious, when the distortions of the coordination polyhedra are analyzed in detail. Thus, a small number of close contacts [ $d(\text{Sb}-\text{S}) < 2.7 \text{ \AA}$ ] between antimony and sulfur are found for both antimony atoms. The discrepancy becomes obvious when the longer contacts are regarded, i.e.,  $2.7 < d(\text{Sb}-\text{S}) < 3.6 \text{ \AA}$ . One antimony cation has six neighbors within this limit; the other one has seven neighbors. By adding  $\text{Li}_2\text{S}$  to  $\text{Sb}_2\text{S}_3$ , the coordination of  $\text{Sb}^{3+}$  cations therein is changed, i.e., all antimony cations take a more similar coordination. Three short distances to sulfur and three longer ones (shorter than 3.6  $\text{\AA}$ ) are observed. Thus, the coordination of antimony in the title compound seems more regular than in  $\text{Sb}_2\text{S}_3$  despite the low symmetry of  $\text{Li}_3\text{Sb}_{11}\text{S}_{18}$ . We propose that the ordering pattern of antimony and lithium results from a low annealing temperature similar as in the case of  $\text{LiSbS}_2$ , which

has an ordered cation distribution at low temperature and perfect disorder at elevated temperature.

A detailed analysis of vibration spectra of the thioantimonate groups in  $\text{Cu}_3\text{SbS}_3$  and in  $(\text{CuI})_2\text{Cu}_3\text{SbS}_3$  showed the significant influence of the so-called secondary bonds between antimony and sulfur atoms in a distance of less than 3.8  $\text{\AA}$  [19]. There are no such “non-bonding” interactions present in  $(\text{CuI})_2\text{Cu}_3\text{SbS}_3$ , and therefore a significant blue-shift of the valence-bond vibrations are found in comparison to  $\text{Cu}_3\text{SbS}_3$ . A similar behavior was found for several thioantimonates(III) both in transition metal chalcogenides with naked counter ions as well as with complex counter ions [20–24]. Unfortunately, we were unable to record reasonable Raman spectra and cannot analyze the bonding situation between antimony and sulfur in this complicated superstructure derived from the rock salt structure type.

## Experimental

### Synthesis

$\text{Li}_3\text{Sb}_{11}\text{S}_{18}$  was synthesized by stoichiometric amounts of  $\text{Li}_2\text{S}$  (99.9%, Alfa Aesar) and  $\text{Sb}_2\text{S}_3$  (Merck). All manipulations were performed in a glove box under an argon atmosphere. The reagents were filled in graphite crucibles, sealed in evacuated silica ampoules, and annealed for 2 weeks at 773 K. Suitable single crystals of  $\text{Li}_3\text{Sb}_{11}\text{S}_{18}$  were separated from the dark-gray inhomogeneous reaction product. The product is air and moisture sensitive.

### Structure determination

Selected single crystals of the title compound were separated from the reaction product and checked for their quality. Diffraction data were collected on an Agilent SuperNova diffractometer with  $\text{MoK}\alpha$  radiation. Data were corrected for Lorentz, and polarization effects, and absorption was corrected numerically [25]. All reflections could be indexed by a triclinic unit cell with a four times larger volume as compared to the structural data given in [2].

The crystal structure was solved by SuperFlip [26] implemented in the Jana2006 program package [27]. By this means, the positions of 11 antimony atoms and of 18 sulfur atoms were obtained. The subsequent refinement using anisotropic displacement parameters for these atoms converged, and then four positions occupied by lithium were obtained from difference-Fourier syntheses. Li1 and Li2 are located on special positions, Li3 and Li4 on general positions. The displacement parameters of Li1–Li3 were refined isotropically,  $U_{\text{eq}}$  (Li4) had to be fixed to a reasonable value

of 0.02. The disorder between Sb and Li as described in [2] was resolved by the four times larger unit cell. Therefore, no disorder had to be taken into account. Finally, the refinement converged to the *R*-values displayed in Table 1.

## References

1. Olivier-Fourcade J, Izghouti L, Maurin M, Philippot E (1983) *Rev Chim Miner* 20:186
2. Olivier-Fourcade J, Maurin M, Philippot E (1983) *Rev Chim Miner* 20:196
3. Huber S, Preitschaft C, Weihrich R, Pfitzner A (2012) *Z Anorg Allg Chem* 638:2542
4. Huber S, Pfitzner A (2015) *Chem Eur J* 21:13683
5. Huber S, Pfitzner A (2014) *Z Anorg Allg Chem* 640:1596
6. Yu DYW, Hoster HE, Batabyal SK (2014) *Sci Rep* 4:4562
7. Park CM, Hwa Y, Sung NE, Sohn HJ (2010) *J Mater Chem* 20:1097
8. Hou H, Jing M, Huang Z, Yang Y, Zhang Y, Chen J, Wu Z, Ji X (2015) *Appl Mater Interfaces* 7:19362
9. Pfitzner A, Kurowski D (2000) *Z Kristallogr* 215:373
10. Puls A, Näther C, Bensch W (2006) *Z Anorg Allg Chem* 632:1239
11. Lühmann H, Rejai Z, Möller K, Leisner P, Ordolff ME, Näther C, Bensch W (2008) *Z Anorg Allg Chem* 634:1687
12. Shannon RD (1976) *Acta Crystallogr A* 32:751
13. Pfitzner A (1994) *Z Anorg Allg Chem* 620:1992
14. Makovicky E, Balic-Zunic T (1995) *Can Mineral* 33:655
15. Pfitzner A (1998) *Z Kristallogr* 213:228
16. Lutz HD, Kuske P, Pfitzner A (1989) *Ber Bunsen-Ges Phys Chem* 93:1340
17. Lutz HD, Pfitzner A, Wickel C (1991) *Solid State Ionics* 48:131
18. Kyono A, Hayakawa A, Horiki M (2015) *Phys Chem Mineral* 42:475
19. Pfitzner A (1997) *Chem Eur J* 3:2032
20. Pfitzner A (2000) *Z Kristallogr* 215:373
21. Schaefer M, Stähler R, Kiebach WR, Näther C, Bensch W (2004) *Z Anorg Allg Chem* 630:1816
22. Möller K, Näther C, Bannwarth A, Bensch W (2007) *Z Anorg Allg Chem* 633:2635
23. Quiroga-González E, Näther C, Bensch W (2009) *Z Naturforsch* 64b:1312
24. Kysliak O, Beck J (2013) *Z Anorg Allg Chem* 639:2860
25. Agilent Technologies XRD Products (2014) *CrysAlisPro*, Version 1.171.37.34
26. Palatinus L, Chapuis G (2007) *J Appl Cryst* 40:786
27. Petricek V, Dusek M, Palatinus L (2014) *Z Kristallogr* 229:345